AJNR

Pontine Tegmental Cap Dysplasia: MR Imaging and Diffusion Tensor Imaging Features of Impaired Axonal Navigation

P. Jissendi-Tchofo, D. Doherty, G. McGillivray, R. Hevner, D. Shaw, G. Ishak, R. Leventer and A.J. Barkovich

AJNR Am J Neuroradiol 2009, 30 (1) 113-119
doi: https://doi.org/10.3174/ajnr.A1305
http://www.ajnr.org/content/30/1/113

ORIGINAL RESEARCH

Pontine Tegmental Cap Dysplasia: MR Imaging and Diffusion Tensor Imaging Features of Impaired Axonal Navigation

P. Jissendi-Tchofo
D. Doherty
G. McGillivray
R. Hevner
D. Shaw
G. Ishak
R. Leventer
A.J. Barkovich

BACKGROUND AND PURPOSE: Malformations of the brain stem are uncommon. We present MR imaging and diffusion tensor imaging (DTI) features of 6 patients with pontine tegmental cap dysplasia, characterized by ventral pontine hypoplasia and a dorsal "bump," and speculate on potential mechanisms by which it forms.

MATERIALS AND METHODS: Birth and developmental records of 6 patients were reviewed. We reviewed MR imaging studies of all patients and DTIs of patient 3. Potential developmental causes were evaluated.

RESULTS: All patients were born uneventfully after normal pregnancies except patient 6 (in utero growth retardation). They presented with multiple cranial neuropathies and evidence of cerebellar dysfunction. Variable hypotonia and motor dysfunction were present. Imaging revealed ventral pontine hypoplasia and mild cerebellar vermian hypoplasia, in addition to an unusual rounded to beaklike "bump" on the dorsal surface of the pons, extending into the fourth ventricle. Color fractional anisotropy maps showed the bump to consist of a bundle of axons directed horizontally (left-right). The bump appeared, on morphologic images, to be continuous with the middle cerebellar peduncles (MCPs), which were slightly diminished in size compared with those in healthy infants. Analysis of the DTI was, however, inconclusive regarding the connections of these axons. The decussation of the MCPs, transverse pontine fibers, and longitudinal brain stem axonal pathways was also abnormal.

CONCLUSIONS: Our data suggest that the dorsal transverse axonal band in these disorders results from abnormal axonal pathfinding, abnormal neuronal migration, or a combination of the 2 processes.

Malformations of the brain stem are very rare and usually result in severe clinical manifestations: notably feeding disorders, impaired swallowing, sensorineural hearing loss, long tract signs, and palsy of cranial nerve V. They have recently been classified into several groups of disorders, including malformations with abnormal brain stem segmentation or segmental hypoplasia, postsegmentation malformations (putative pathfinding or migration abnormalities), and malformations associated with abnormal cortical organization.[1] We report MR imaging and diffusion tensor imaging (DTI) findings of an unusual malformation characterized by pontine hypoplasia with ectopic dorsal transverse pontine fibers in 6 patients presenting with the clinical manifestations of multiple cranial nerve palsies and variable long tract signs. Similar MR imaging features have been described as pontocerebellar hypoplasia,[2] Möbius syndrome,[3] and, recently, a new malformation called "pontine tegmental cap dysplasia."[4] We discuss the clinical presentation, morphologic abnormalities, and the potential underlying mechanisms that may cause this interesting malformation.

Received May 22, 2008; accepted after revision August 4.

From the Neuroradiology section (P.J.-T., A.J.B.), Department of Radiology, University of California, San Francisco, Calif; Service de Neuroradiologie (P.J.-T.), Hôpital Salengro, CHRU Lille, Lille, France; Neuroradiology section (P.J.-T.), Department of Radiology, Erasme Hospital, Brussels, Belgium; Division of Genetics and Developmental Medicine (D.D.), University of Washington, Children's Hospital and Medical Center, Seattle, Wash; Genetic Health Services (G.M.), Murdoch Children's Research Institute, Royal Children's Hospital, Melbourne, Australia; Neurological Surgery/Neuropathology (R.H.), University of Washington School of Medicine, Seattle Children's Hospital Research Institute, Seattle, Wash; Department of Radiology (D.S., G.I.), Children's Hospital and Medical Center, Seattle, Wash; and Department of Child Neurology (R.L.), Royal Children's Hospital, Parkville, Australia.

Please address correspondence to Patrice Jissendi, MD, Radiology Department, Erasme Hospital, Route de Lennik 808, B-1070 Brussels, Belgium; e-mail: jissendi@gmail.com

DOI 10.3174/ajnr.A1305

Materials and Methods

Six patients were found in different centers, where they were evaluated in infancy for delayed development or failure to thrive. All were referred for routine brain MR imaging after pediatric neurologic examination disclosed multiple cranial neuropathies. No family history of brain malformation was obtained in any of the patients. Clinical data available for each patient are summarized in Table 1.

All patients were examined by MR imaging at 1.5T, including axial, coronal, and sagittal T1-weighted (from direct acquisitions with 4-mm section thickness or sagittal 3D spoiled gradient-recalled-echo and magnetization-prepared rapid acquisition of gradient echo sequences [SPGR, MPRAGE] with coronal and axial reconstructions) and/or T2-weighted images (4-mm section thickness). Patient 3 and a neurologically healthy control, matched for age, underwent DTI performed on a Trio 3T MR imaging scanner (Siemens, Erlangen, Germany) sampling the data in 30 directions. Other parameters were the following: TE = 96 ms; TR = 6600 ms; b = 1000 s/mm^2; FOV = 240 × 240 mm; matrix = 128 × 128; section thickness = 2 mm; number of averages = 2; bandwidth = 1396 Hz/pixel with generation of cross-sectional directionally encoded fractional anisotropy (FA) color maps.

Results

All imaging findings are summarized in Table 2. Anatomic images in all patients revealed a small pons with a variably shaped band of white matter coursing like an exophytic mass along its dorsal superior aspect (Fig 1). In patient 4, this band had a beaklike appearance, but in the other patients, it was more roundly shaped, smaller and smoother (caplike). These

Table 1: Patient data

	Patient 1	Patient 2	Patient 3	Patient 4	Patient 5	Patient 6
Sex	M	M	M	F	F	F
Parent consanguinity	No	No	No	NA	No	No
Family history	Autosomal dominant retinitis pigmentosa (father, paternal aunt, paternal grand-father)	No significant history	NA	NA	No neurologic or developmental disorders, mother with hypothyroidism	No neurologic or developmental disorders, sister with interrupted aortic arch, 2nd cousin with VSD
Siblings	Twin brother, normal	Female sibling, normal	NA	NA	NA	None
Pregnancy	Twin pregnancy (monozygotic with single placenta)	Singleton pregnancy	NA	NA	Singleton pregnancy	Singleton pregnancy, IUGR
Antenatal Imaging	US at 20 w: cerebellar hypoplasia	US at 18 w: cerebellar hypoplasia; at 21w: scoliosis with 2 hemivertebrae	NA	NA	NA	NA
Delivery	Elective cesarian birth at 38 w	Elective cesarian birth at 37w	NA	Normal, delayed cry	Cesarean birth for maternal hypertension at 38 w	Cesarean birth for fetal distress at 34 w
Birth W/L/HC	2580 g/47 cm/33 cm	2450 g/NA/31.8 cm	2512 g/47.2 cm/31.9 cm	Low weight	2850 g/NA/32.5 cm	1493 g/NA/NA
Cranial nerve involvement	Bilateral V palsies, bilateral facial weakness (VII), bilateral sensorineural hearing loss (VIII) diagnosed at 18 m	Partial V palsy, possible VI palsy; lower facial weakness, profound high frequency sensorineural hearing loss, VII and VIII palsies	Moderate left hearing loss (VIII)	Bilateral partial V palsies, bilateral VII palsies, bilateral VIII palsies	Bilateral severe sensorineural hearing loss	Bilateral severe sensorineural hearing loss, bilateral absence of the vestibular nerves on MRI, bilateral VII palsy, bilateral V
Ocular abnormalities	Oculomotor apraxia, no nystagmus; corneal ulcers	Poor visual fixing, apparent inability to close the eyes, severe corneal drying and right corneal ulcer	Absent corneal sensation bilaterally, vertical nystagmus, abnormal gaze-holding, smooth pursuit, saccades, no vestibular ocular reflexes	Bilateral corneal opacities	Unilateral corneal abrasion leading to corneal opacity, near-absent voluntary eye movements, esotropia requiring bilateral rectus muscle recession	Decreased corneal sensation, impaired smooth pursuit but otherwise normal eye movements
Swallowing	Impaired	Impaired	Impaired	Impaired	Impaired	Impaired
Feeding	Poor, nasogastric tube followed by gastrostomy at 5 m	Feeding difficulties requiring nasogastric tube	Feeding difficulties	NA	Gastrostomy at 4 m	Feeding difficulties improved with age
Cerebellar symptoms	Ataxia	Abnormal movements	Head titubation, uncoordinated movements	Ataxia	Head titubation	Ataxia
Pyramidal symptoms	NA	Hypotonia	Mild motor delay	Normal tone and bulk, brisk reflexes	Bilateral ankle clonus	Mildly increased lower extremity tone, brisk reflexes
Other neurologic or behavioral findings	None	Mildly dysmorphic features with low set and simple ears, a broad nasal root, a small upturned nose, hypoplastic alar nasae, a long smooth upper lip and mild retrognathia	Bangs forehead on surfaces	NA	None	Unknown
Extracranial anomalies	Thoracic scoliosis, numerous hemivertebrae	Vertebral segmentation anomalies on the thoracic and lumbar spine, cocked first toe with a Y-shaped configuration of the second and third toes with minimal syndactyly, horseshoe configuration of the kidneys	None	Erythematous maculopapular skin rash over face, trunk, and limbs	None	Severe narrowing of the auditory canals, membranous VSD, submucous cleft palate, bilateral inguinal hernias, obstructive sleep apnea
Global development	Developmental delay noted from early infancy	Failure to thrive	NA	NA	Severe developmental delay	Mild developmental delay: walks with a walker, uses many signs, some ability to read and type
EEG	PSG: recurrent central apneas, hypoventilation during REM sleep	Seizures with clonic upper limb movements and facial twitching at 5 w responding to phenobarbital	Excessive multifocal sharp waves, without sustained epileptiform activity	NA	Normal	NA
Blood examination	Lysosomal enzymes, very-long-chain fatty acids; serum lactate and pyruvate, Transferrin isoforms and plasma amino acids, normal	Total glycosaminoglycan level slightly elevated	NA	NA	Normal transferrin, deficient glycoprotein testing, mildly elevated CK and liver transaminases	Normal transferrin, deficient glycoprotein testing
CSF examination	Lactate and pyruvate slightly elevated	Nonspecific elevation of amino acids	NA	NA	NA	NA
Urine examination	NA	Organic and amino acid levels, normal	NA	NA	Urine organic acids, plasma amino acids, normal	Urine metabolic screen normal
Karyotype	*46XY*	*46XY*	NA	NA	*46XX*, normal VCFS and subtelomeric FISH testing	*46XX*, normal VCFS and subtelomeric FISH testing
Latest data	NA	Status epilepticus, hypoglycemia, metabolic acidosis, coagulopathy, and decreased pain response; died at 6 m from parainfluenza pneumonia	5 months old	6 months old	Died at 2 years of age from unknown cause	10 years old

Note:—NA indicates not available; w, weeks; m, months; W, weight; L, length; HC, head circumference; US, ultrasound; PSG, polysomnography; REM, rapid eye movement; VSD, ventricular septal defect; IUGR, inutero growth retardation; MRI, MR imaging; VCFS, velo-cardio facial syndrome; FISH, fluorescence in-situ hybridization; CK, creatine kinase.

Table 2: MR imaging findings in all patients and DTI findings in patient 3

	Patient 1	Patient 2	Patient 3	Patient 4	Patient 5	Patient 6	DTI Findings in Patient 3
Cerebellar hemispheres	Small	Small	Normal appearance	Small	Hypoplastic and dysplastic	Small	
Vermis	Moderately hypoplastic	Hypoplastic and dysplastic	Normal appearance	Hypoplastic and dysplastic	Hypoplastic and dysplastic	Hypoplastic	
Fourth ventricle	Slightly enlarged	Slightly enlarged	Normal, partially occupied by the cap	Slightly enlarged	Normal, partially occupied by the cap	Slightly enlarged	
SCP	Elongated	Elongated	Elongated	Elongated	Elongated	Elongated	Elongated, no decussation
MCP	Small	Small	Small	Small	Small	Small	Small, joined by the EDTB
ICP	Un	Un	Un	Small	Un	Un	Un
Pons	Hypoplastic, flattening of the ventral aspect, dorsal cap, "horizontal cleft" deformity	Hypoplastic, flattening of the ventral aspect, dorsal cap, "horizontal cleft" deformity	Hypoplastic, flattening of the ventral aspect, dorsal cap, "horizontal cleft" deformity	Hypoplastic, flattening of the ventral aspect, dorsal cap, "horizontal cleft" deformity	Hypoplastic, flattening of the ventral aspect, dorsal cap, "horizontal cleft" deformity	Hypoplastic, flattening of the ventral aspect, dorsal cap, "horizontal cleft" deformity	Ectopic dorsal transverse bundle or tegmental cap, descending long tracts located ventrally to the EDTB
Pontine-mesencephalon junction (isthmus)	Thin	Thick	Thick	Thick	Thick	Thick	
Cerebrum	Normal appearance	Normal appearance	Normal appearance	Normal appearance	Normal appearance	Normal appearance	
Corpus callosum	Dysmorphic	Hypoplastic	Thin	Hypoplastic	Hypoplastic	Dysmorphic	

Note:—EDTB indicates ectopic dorsal transverse bundle; Un, unidentifiable; DTI, diffusion tensor imaging; SCP, superior cerebellar peduncles; MCP, middle cerebellar penduncles; ICP, inferior cerebellar peduncles.

fibers appeared continuous with the middle cerebellar peduncles on coronal MR images (Fig 2*A*). In some patients, particularly patient 4 (Fig 1*D*), the pons appeared extremely thin immediately caudal to the band. Additional brain stem anomalies included a short mesencephalon-pontine junction (isthmus) that was thin in patient 1, and short and thickened in the others (Fig 1). In most cases, the 4th ventricle was partially occupied by the dorsal band (Fig 1*B–E*). The course of the superior cerebellar peduncles (SCPs) was somewhat lateral in position in patients 1 (Fig 2*B*) and 4. The middle cerebellar peduncles (MCPs) were quite small (Fig 2*D*), and the ventral pons was flattened. The medulla was small, and in patients 1 and 4, it appeared elongated (Fig 1). The inferior cerebellar peduncles (ICPs) were quite small in patient 4 and could not be identified in the others. The cerebellar vermis was normal in patient 3 and small in patients 1 and 6, whereas it was small with abnormal orientation of fissures in patients 2, 4, and 5 (Fig 1*C*, *-D*). The cerebellar hemispheres were small in patients 1, 2, 4, and 6. Axial sections showed hypoplasia of the inferior olives (not shown).

Relatively minor supratentorial anomalies were observed. The corpus callosum (CC) was dysmorphic in patients 1 and 6 but was thin in patient 3 and hypoplastic in the others. Cerebral hemispheres, olfactory bulbs, orbits, optic pathways, hypothalamic areas, and pituitary glands were structurally normal. There was no evidence of a supratentorial cortical malformation in any of the patients. Pineal cysts were found in patients 1 and 3, the latter showing, in addition, a Rathke cleft cyst; these were considered to be incidental findings. Segmentation anomalies of the spinal column, with associated scoliosis, were found in 2 patients. Orbits, calvaria, skull base, and visualized inner and middle ear structures appeared normal in all patients.

FA maps and fiber tractography were obtained in patient 3 (Fig 3) and were compared with studies obtained in the control patient. Cross-sectional FA images verified the impression from the anatomic images that the MCPs were small. The decussation of the MCPs and the fibers to the pontine nuclei were absent at the level of the upper pons, likely explaining the decreased size of the ventral pons. At this same level, an abnormal transverse bundle of axons crossed the midline in the dorsalmost pons, extending from 1 MCP to the other to form the pontine "cap." On the FA and tractography images, these fibers were not obviously continuous with any white matter bundle; indeed, they appeared to terminate at the sites of crossing of the craniocaudally oriented SCPs (Fig 3*B*, *-C*). The SCPs appeared elongated and running laterally. Their decussation was not visible in its normal midbrain location. The ICPs were not visible. Two tracts of longitudinal axons were located in the anterior pons, at the sites normally occupied by the corticospinal and corticopontine tracts, though the size of these bundles of axons was smaller than those seen in the healthy control. It could not be determined whether the dorsal longitudinal axonal pathways (the median longitudinal fasciculus, the medial and lateral lemnisci, etc) were absent or included in these more ventral bundles.

Discussion

Malformations of the brain stem are not well described in the medical literature. One reason is that the brain stem is poorly

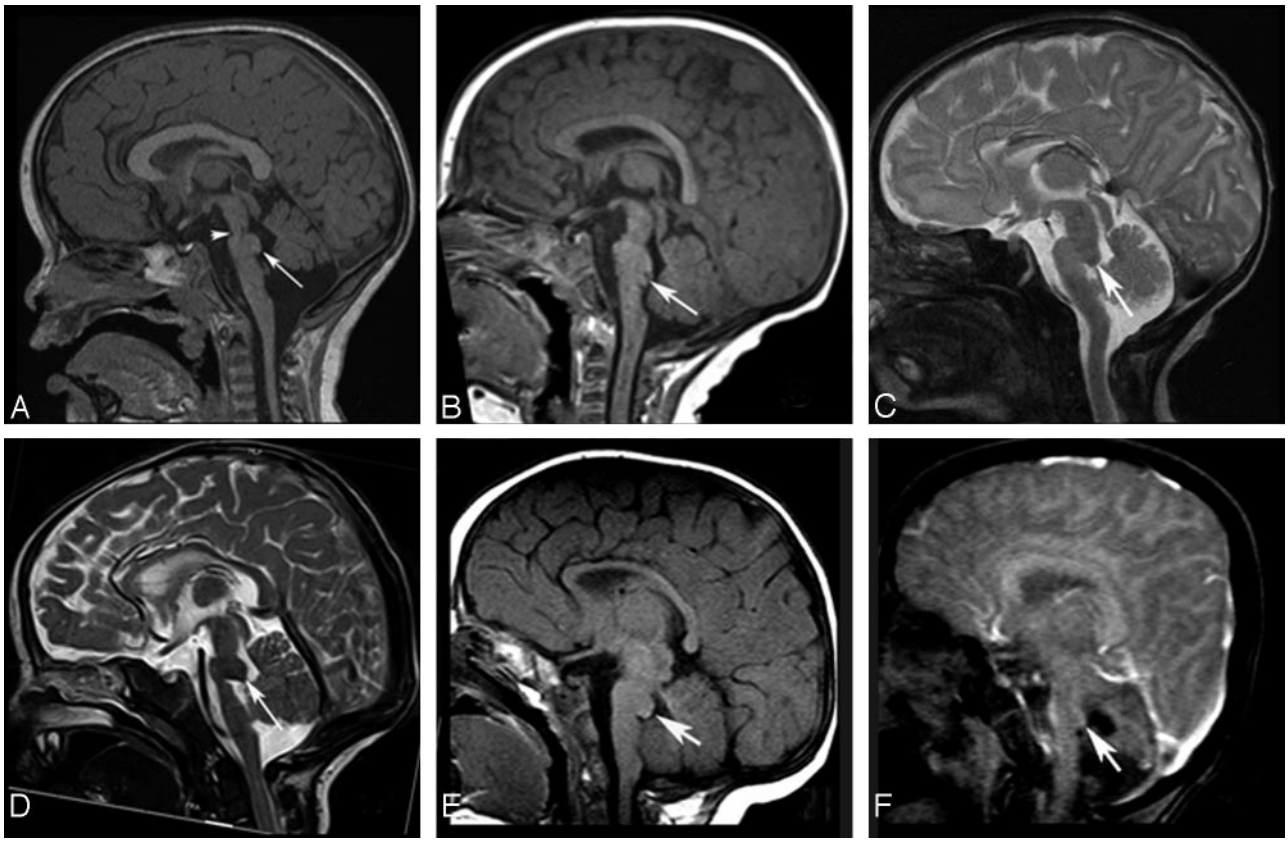

Fig 1. *A* and *B*, Midsagittal T1-weighted images (T1WIs) in patients 1 and 3 show flattening of the ventral pons, thinning of the isthmus (*arrowhead, A*), dysmorphism of the dorsal upper pons (caplike) bulging (*long arrows*) and protruding in the fourth ventricle (*B*). The vermis is hypoplastic in *A*. *C* and *D*, Midsagittal T2WIs in patients 2 and 4 show the same findings as in *A* and *B*, with slightly different patterns (beaklike shape in *D*) (*long arrow*). In both cases, the vermis is hypoplastic and dysplastic and the CC is hypoplastic. The CC is dysmorphic in patient 3 (*B*) and thin in patient 4 (*D*). *E* and *F*, Midsagittal T1- and T2WIs for patients 5 and 6 show the tegmental cap with hypoplastic (*E* and *F*) and dysplastic (*E*) vermis. *F*, Fourth ventricle is slightly enlarged. The CC is hypoplastic in *E* and dysmorphic in *F*.

evaluated by both pathology and neuroimaging. Pathologic analysis of the malformations is inhibited by difficulty in evaluating the axonal pathways using traditional techniques of brain cutting. Early MR imaging was hampered by long imaging times, artifacts generated by rapid CSF flow in the perimedullary and peripontine cisterns, and the inability to differentiate nuclei from white matter pathways. Only recently, with the development of parallel imaging techniques (to improve signal intensity–to-noise ratio and the speed of imaging), stronger gradients (to allow thinner imaging sections), and DTI (to allow evaluation of white matter tracts) has MR imaging begun to be useful in the evaluation of brain stem disorders.[5-7] We report here the MR imaging evaluation of 6 patients and DTI of 1 with an unusual malformation of the pons, which may be more common than generally realized.

Similar MR imaging findings have been previously reported[2,3] but were not recognized as a unique entity until Barth et al[4] described 4 cases, which they called "pontine tegmental cap dysplasia." It has been reported in sporadic male and female cases without affected siblings or consanguinity. Although autosomal recessive inheritance cannot be excluded, new dominant mutations, such as submicroscopic chromosomal rearrangements, may be a more likely mechanism.[8] To date, to our knowledge, none of the published patients have been evaluated with tiling-path or high-attenuation oligonucleotide comparative genomic hybridization arrays.

Our morphologic and DTI analyses of the affected brain

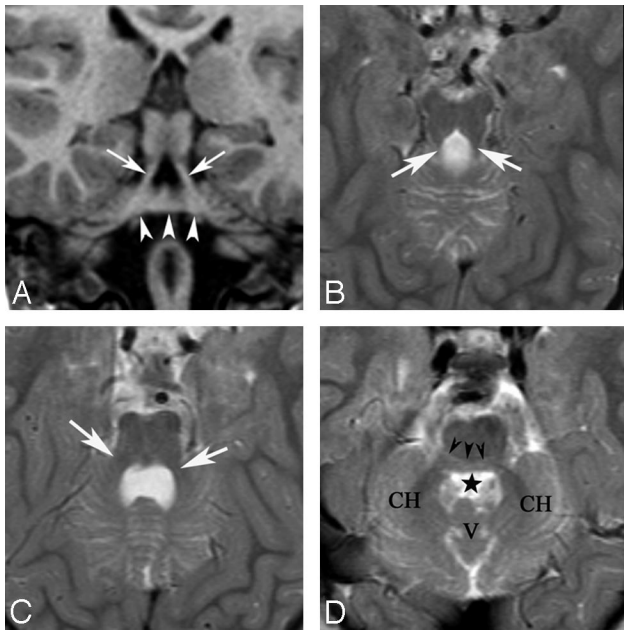

Fig 2. Patient 1: *A* and *B*, Coronal T1-weighted images and axial T2-weighted images (T2WIs) show the "molar tooth" appearance of the elongated SCPs running laterally (*arrows*) and the dorsal band crossing the midline and likely joining the MCPs (*arrowheads*). *C*, Axial T2WI at the level of the MCPs, which appear small (*white arrows*). *D*, Axial T2WI at the level of middle pons. A "horizontal cleft" is visible, outlined by *black arrowheads*. The *black star* indicates the fourth ventricle. Note the small size of cerebellar hemispheres (CH) and the hypoplastic vermis (V).

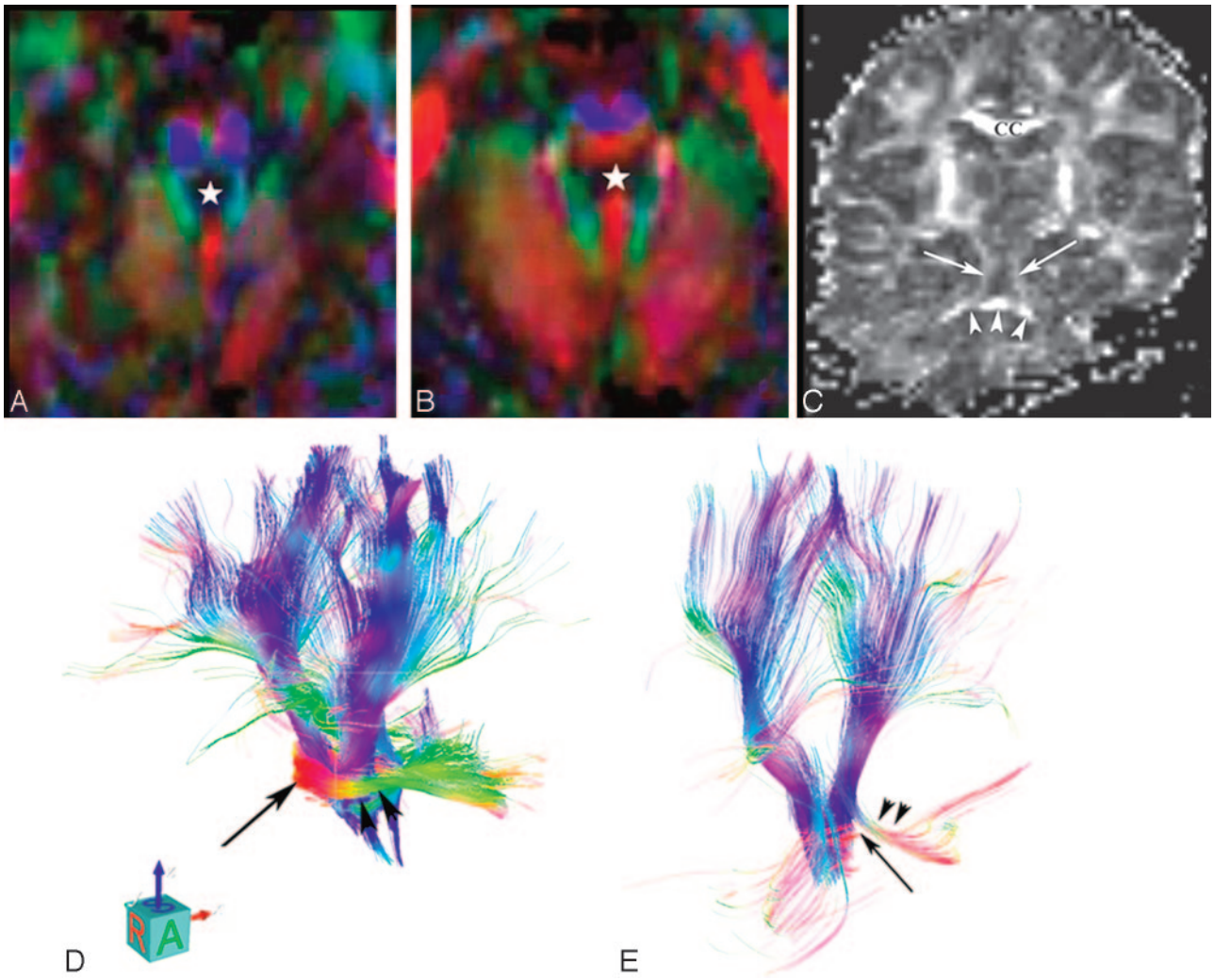

Fig 3. Patient 3: *A* and *B*, Color FA cross-sectional images show elongation of the SCP (green).The *white star* indicates the fourth ventricle. Descending long tracts (corticospinal and corticopontine) appear in blue. The ventral and middle transverse pontine fibers are missing; the SCP decussation is not visible. *B*, The ectopic bundle of fibers appears in red at the dorsal aspect of the pons and seems not to connect the MCPs visible laterally. *C*, Coronal FA image shows the elongated SCPs running laterally (*arrows*); the dorsal band (*arrowheads*) crossing the midline may join either the SCPs vertically or the MCPs horizontally. *D* and *E*, 3D projections of tractography. In the control (*D*), ventral transverse fibers are clearly seen (*black arrow*) and the MCPs are of normal size (*arrowheads*). In patient 3 (*E*), long descending tracts and the MCPs appear smaller (*arrowheads*). The ectopic dorsal pontine fibers are visible (*long arrow*) and are not seen to definitely connect the MCP (*arrowheads*).

stem gave results that are similar to those reported by Barth et al.[4] The band on the dorsal aspect of the upper pons appears to be a bundle of transversely oriented fibers (red on the color FA map, Fig 3*B*). Although the axons appear to be continuous with the MCPs on the morphologic image (Fig 2*A*, -*D*), this impression is not confirmed by the color FA map, where the fibers seem to terminate when they reach the SCPs (Fig 3*C*, -*D*). However, connectivity may not be demonstrated because of the technical limitations of DTI (tractography terminates when either the FA or the angle of the tract falls below a specified threshold). Therefore, just as the corticospinal tracts often appear to terminate in the cerebrum immediately above the lateral ventricles, where the perpendicular callosal fibers cross and reduce intravoxel anisotropy to nearly zero, the pontine cap axons, coursing horizontally, may appear to terminate when crossing the craniocaudally oriented SCPs.

Tractography, by using higher angular resolution diffusion techniques that can better follow axons through regions of complex axonal anatomy (Q-ball imaging, spheric deconvolution, or persistent angular structure) might better resolve these tracts and determine the full course of the pathways in which the band is involved.[5-7] Another possibility for the origin of the axons is a misorientation of the descending pathway of dorsal long tracts: medial lemniscus, lateral lemniscus, medial longitudinal fasciculus, posterior longitudinal fasciculus, central tegmental, trigeminothalamic, spinothalamic, and tectospinal tracts.[1,9] Neurologic testing of these tracts was not possible in our patient because of his young age, but some of our other patients, and those described by Barth et al,[4] did show some abnormalities of horizontal gaze.

The long tracts visible in the ventral pons at the level of the dorsal "cap" corresponded reasonably well, in terms of location and their rostral pathway, to the corticospinal and corticopontine tracts but were smaller than those in the control. The smaller size of the tracts might explain, at least partly, the motor problems observed in our patients. Three other major findings were identified on the color FA map of our patient: absence of the SCP decussation, markedly diminished size of

the MCPs, and poor or nonvisualization of the ICPs. These observations suggest an impairment of axonal navigation, with absence or diminished number of axons, abnormal course (failure to cross the midline), and ectopic white matter fibers within the pons, as 1 possible cause of this malformation. Axonal guidance molecules such as netrins, ephrins, semaphorins, and their receptors may, therefore, be candidates for causative molecules.[10-18]

Migrating axons navigate by responding to chemical guidance cues via multiple membrane-associated signaling molecules. Studies of animal models have helped in identifying the molecules involved in this process. *Netrin-1* interacts with *DCC* (attraction and sometimes repulsion) and with *UNC-5* (repulsion) family receptors, which are located on the surface of the growth cone. The guidance response is assured by multiple cytoskeletal proteins.[14] An aberrant trajectory could thus result from an erroneous extracellular target or a defect in proteins of the cytoskeleton. Axon guidance by netrins needs to be regulated in mice by a signaling system from the midline mediated by *Slit* (*Sli*) and its receptors *Robo1*, *2,* and *3*.[19,20] An additional signaling system for *Netrin* (*Net*) uses the receptor *Frazzled* (*Fra*), which functions as a midline attractant for the tracts at the point of midline crossing.[20] A loss of *Net-Fra* or overexpression of *Sli-Robo* function that results in long tracts shifting far from the midline could explain the absence of SCP decussation and the presence of a molar toothlike midbrain appearance in some of our patients, as well as the dorsal transverse axonal band.

The presence of a molar toothlike midbrain might also suggest that the primary problem in this disorder is one involving ciliary proteins, as appears to be the case in Joubert syndrome and related disorders (the "molar tooth malformations"),[21-23] in which the decussation of both the SCPs and the corticospinal tracts seems to be affected.[24] No renal cysts or cystic degeneration has, as yet, been reported in patients with dorsal transverse pontine bands, but the kidneys may not yet have been adequately assessed. If extra-central nervous system anomalies, such as retinal dystrophy, cystic renal disease, and polydactyly, were to be discovered, mutations affecting ciliary proteins might be revealing.

Abnormal migration of pontine neurons might also be implied by the flattened pons and by the aberrant origin of the transverse tract (presumably arising from ectopic pontine neurons) in the tegmentum. One of the *Netrin-1* receptors, *Unc5h3*, is also involved in neuronal-migration guidance.[11] Thus, a loss of *Unc5h3* function may result both in abnormal neuronal migration and axonal navigation impairment. Moreover, developing neurons undergo apoptosis if synaptic connections are not established. Therefore, we can hypothesize that impaired proliferation or abnormal migration of cortical and pontine neurons might be responsible for the small size of the ventral longitudinal tracts (corticospinal and corticopontine) and one of the reasons for the flattening of the ventral pons and, in some cases as well, for the small/dysplastic vermis and small cerebellar hemispheres (patient 1). Indeed, a unifying feature in this disorder appears to be the involvement of rhombic lip (RL) derivatives: pontine nuclei, inferior olivary nuclei, cerebellar cortex (granule cells), and deep cerebellar nuclei; all arise from RL. During normal development, the transverse pontine fibers normally connect the pontine nuclei

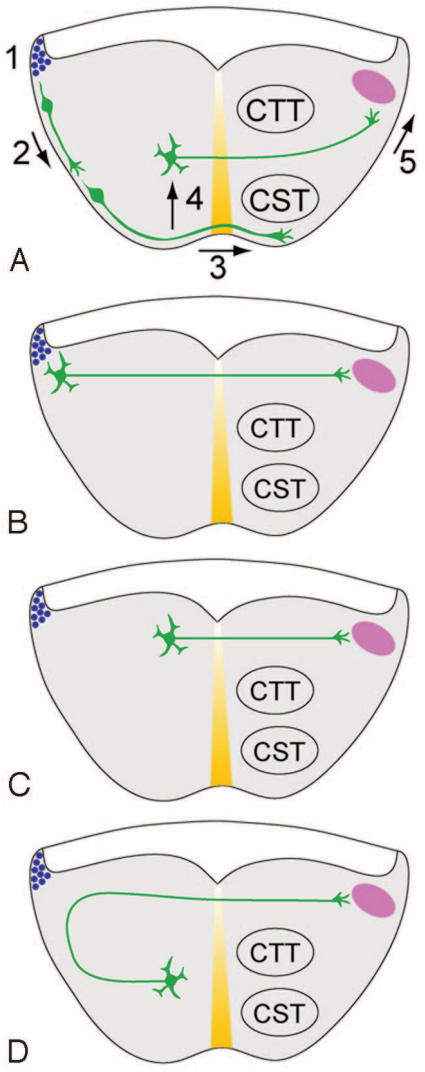

Fig 4. Hypotheses to explain the aberrant dorsal position of transverse pontine fibers. *A,* Normal development. 1) Pontine gray neurons are produced from progenitors in the rhombic lip (*blue circles*). 2) Newly generated neurons migrate toward the ventral midline (yellow), the "anterior extramural migratory stream" of Altman and Bayer.[25] 3) Axonal growth cones cross the ventral midline, leaving most neuronal cell bodies uncrossed.[26] 4) Cell bodies migrate toward the ventricle along radial glia.[27] 5) Axonal growth cones migrate into the MCP (pink). The transverse pontine fibers are sandwiched between the concurrently growing corticospinal tract (CST) and central tegmental tract (CTT). *B,* Hypothesis 1: Decreased ventral migration (step 2) leaves the pontine gray neurons scattered along the lateral pontine surface. Axonal growth cones cross the midline directly toward the contralateral MCP. *C,* Hypothesis 2: Increased radial migration (step 4) deposits pontine neurons near the ventricular surface of the pontine tegmentum. *D,* Hypothesis 3: Normal migration of pontine neurons. Note abnormal axon guidance away from the ventral surface, followed by midline crossing and attraction toward the MCP.

to the contralateral cerebellar cortex via the MCPs (Fig 4).[25-27] The pontine cap could form by reduced ventral migration of pontine nuclei, followed by effective axon migration across the midline, leaving connections with the cerebellar cortex somewhat preserved. Another hypothesis might be that increased radial migration of pontine nuclei would result in pontine gray neurons being located near the ventricular surface of the pontine tegmentum and the consequent aberrant position of their axons. Finally, normal migration of pontine neurons followed by abnormal axon guidance away from the ventral surface of the pons is another plausible hypothesis (Fig 4*D*). Ultimately, gross and microscopic neuropathologic analysis of

autopsy specimens or development of an animal model will be required to clarify this question. Barth et al[4] performed no pathologic analysis of their patients and found no pathogenic mutations in the coding regions of the *NTN1* and *DCC* genes in their patients.[4] They also concluded that *Robo3* mutations are unlikely to be causative of this complex malformation on the basis of the lack of similarity to the human disorder, horizontal gaze palsy, with progressive scoliosis known to be caused by these mutations.[28]

Another clue to the molecular etiology of this condition may come from the anomalies of vertebral segmentation found in 2 of our patients and 3 of the patients reported by Barth et al.[4] A combination of hindbrain anomalies, cranial nerve dysfunction, and vertebral anomalies may suggest changes in function of the highly conserved *Hox* genes, which encode transcription factors within a deoxyribonucleic acid–binding homeodomain. The expression of genes from paralogous clusters of *Hox* genes in the vertebrate presomitic mesoderm results in the segmental formation of somites, from which the vertebrae derive.[29] Similar *Hox* gene expression in the developing vertebrate hindbrain, from which the pons, medulla, and cerebellum develop, results in the segmental formation of rhombomeres, the patterning of cranial nerves, and their distribution to structures of the head and neck.[30,31] Thus, abnormalities of *Hox* genes could be another mechanism by which these malformations develop. Again, careful pathologic analysis and development of animal models may be useful in gaining a better understanding of the causative mechanisms.

Conclusions

We report 6 new cases of pontine tegmental cap dysplasia, raising the number of all published cases of this malformation to 10.[2-4] The large number of reports published recently suggests that the disorder may be more common than generally realized and may have been misdiagnosed as pontocerebellar hypoplasia or Möbius syndrome. Some of us are currently reviewing all of our pontocerebellar hypoplasia cases to determine the proportion that may actually have pontine cap dysplasia. Our findings support the hypothesis of a complex pontine malformation featuring an impairment of axonal navigation or migration of neurons generated in the rhombic lips. The etiology is unknown, but likely to be genetic. Further clinical description and neuroimaging, in combination with neuropathology and animal studies, will be required to understand this new entity.

Acknowledgment

We thank Dr. Lee Coleman for referral of patient 2.

References

1. Barkovich AJ, Millen KJ, Dobyns WB. **A developmental classification of malformations of the brainstem.** *Ann Neurol* 2007;62:625–39
2. Maeoka Y, Yamamoto T, Ohtani K, et al. **Pontine hypoplasia in a child with sensorineural deafness.** *Brain Dev* 1997;19:436–39
3. Ouanounou S, Saigal G, Birchansky S. **Möbius syndrome.** *AJNR Am J Neuroradiol* 2005;26:430–32
4. Barth PG, Majoie CB, Caan MW, et al. **Pontine tegmental cap dysplasia: a novel brain malformation with a defect in axonal guidance.** *Brain* 2007;130(pt 9):2258–66
5. Tuch DS, Wisco JJ, Khachaturian MH, et al. **Q-ball imaging**. *Magn Reson Med* 2004;52:1358–72
6. Tournier JD, Calamante F, Gadian DG, et al. **Direct estimation of the fiber orientation density function from diffusion-weighted MRI data using spherical deconvolution.** *Neuroimage* 2004;23:1176–85
7. Jansons KM, Alexander DC. **Persistent angular structure: new insights from diffusion MRI data—dummy version.** *Inf Process Med Imaging* 2003;18: 672–83
8. Stankiewicz P, Lupski JR. **Genome architecture, rearrangements and genomic disorders.** *Trends Genet* 2002;18:74–82
9. Fitzgerald MJT. **Neuroanatomy Basic and Applied.** Oxford, UK: Ballière Tindall; 1985:84–93
10. Serafini T, Colamarino SA, Leonardo ED, et al. **Netrin-1 is required for commissural axon guidance in the developing vertebrate nervous system.** *Cell* 1996;87:1001–14
11. Barallobre MJ, Pascual M, Del Río JA, et al. **The netrin family of guidance factors: emphasis on netrin-1 signalling.** *Brain Res Brain Res Rev* 2005;49;22–47. Epub 2005 Jan 15
12. Deiner MS. **Netrin-1 and DCC mediate axon guidance locally at the optic disc: loss of function leads to optic nerve hypoplasia.** *Neuron* 1997;19:575–89
13. Astic L, Pellier-Monnin V, Saucier D, et al. **Expression of netrin-1 and netrin-1 receptor, DCC, in the rat olfactory nerve pathway during development and axonal regeneration** *Neuroscience* 2002;109:643–56
14. Finger JH, Bronson RT, Harris B, et al. **The netrin 1 receptors Unc5h3 and Dcc are necessary at multiple choice points for the guidance of corticospinal tract axons.** *J Neurosci* 2002;22:10346–56
15. Inatani M. **Molecular mechanisms of optic axon guidance.** *Naturwissenschaften* 2005;92:549–61. Epub 2005 Oct 12
16. Bhat KM, Gaziova I, Krishnan S. **Regulation of axon guidance by slit and netrin signaling in the Drosophila ventral nerve cord.** *Genetics* 2007;176:2235–46. Epub 2007 Jun 11
17. Sibbe M, Taniguchi M, Schachner M, et al. **Development of the corticospinal tract in semaphorin3a- and CD24-deficient mice.** *Neuroscience* 2007;150;898–904. Epub 2007 Oct 18
18. Mann F, Rougo G. **Mechanisms of axon guidance: membrane dynamics and axonal transport in semaphorin signaling.** *J Neurochem* 2007;102:316–23
19. Jen JC, Chan WM, Bosley TM, et al. **Mutations in a human ROBO gene disrupt hindbrain axon pathway crossing and morphogenesis.** *Science* 2004;304: 1509–13. Epub 2004 Apr 22.
20. Devine CA, Key B. **Robo–Slit interactions regulate longitudinal axon pathfinding in the embryonic vertebrate brain**. *Dev Biol* 2008;313:371–83. Epub 2007 Nov 7.
21. Mykytyn K. **Clinical variability in ciliary disorders.** *Nat Genet* 2007;39:818–19
22. Yachnis AT, Rorke LB. **Cerebellar and brainstem development: an overview in relation to Joubert syndrome.** *J Child Neurol* 1999;14:570–73
23. Parisi MA, Doherty D, Chance PF, et al. **Joubert syndrome (and related disorders) (OMIM 213300).** *Eur J Hum Genet* 2007;15:511–21
24. Gleeson JG, Keeler LC, Parisi MA, et al. **Molar tooth sign of the midbrain-hindbrain junction: occurrence in multiple distinct syndromes.** *Am J Med Genet A* 2004;125:125–34
25. Altman J, Bayer SA. *Development of the Cerebellar System.* Boca Raton, Fla: CRC Press; 1997
26. Marillat V, Sabatier C, Failli V, et al. **The slit receptor Rig-1/Robo3 controls midline crossing by hindbrain precerebellar neurons and axons.** *Neuron* 2004;43:69–79
27. Kawauchi D, Taniguchi H, Watanabe H, et al. **Direct visualization of nucleogenesis by precerebellar neurons: involvement of ventricle-directed, radial fibre-associated migration.** *Development* 2006;133:1113–23
28. Bosley TM, Salih MAM, Jen JC, et al. **Neurologic features of horizontal gaze palsy and progressive scoliosis with mutations in ROBO3.** *Neurology* 2005;64:1196–203
29. Wellik DM. **Hox patterning of the vertebrate axial skeleton.** *Dev Dyn* 2007;236:2454–63
30. Gavalas A, Studer M, Lumsden A, et al. **Hoxa1 and Hoxb1 synergize in patterning the hindbrain, cranial nerves and second pharyngeal arch.** *Development* 1998;125:1123–36
31. Gavalas A, Ruhrberg C, Livet J, et al. **Neuronal defects in the hindbrain of Hoxa1, Hoxb1 and Hoxb2 mutants reflect regulatory interactions among these Hox genes** *Development* 2003;130:5663–79. Epub 2003 Oct 1